Journal of Supramolecular Structure 9:537–554 (1978)
Normal and Abnormal Red Cell Membranes 311–328

Membrane Alterations in Irreversibly Sickled Cells: Hemoglobin–Membrane Interaction

Lawrence S. Lessin, Joseph Kurantsin-Mills, Charles Wallas, and Henri Weems

Division of Hematology and Oncology, Department of Medicine (L.S.L., C.W., H.W.); and Department of Physiology (J.K.-M.); George Washington University Medical Center, Washington, DC 20037

Irreversibly sickled cells (ISCs) are sickle erythrocytes which retain bipolar enlongated shapes despite reoxygenation and owe their biophysical abnormalities to acquired membrane alterations. Freeze-etched membranes both of ISCs produced in vitro and ISCs isolated in vivo reveal microbodies fixed to the internal (PS) surface which obscure spectrin filaments. Intramembranous particles (IMPs) on the intramembrane (PF) surface aggregate over regions of subsurface microbodies. Electron microscopy of diaminobenzidine-treated ISC ghosts show the microbodies to contain hemoglobin and/or hemoglobin derivatives. Scanning electron microscopy and freeze-etching demonstrate that membrane–hemoglobin S interaction in ISCs enhances the membrane loss by microspherulation. Membrane-bound hemoglobin is five times greater in in vivo ISCs than non-ISCs, and increases during ISC production, paralleling depletion of adenosine triphosphate. Polyacrylamide gel electrophoresis of ISC membranes shows the presence of high-molecular-weight heteropolymers in the pre–band 1 region, a decrease in band 4.1 and an increase in bands 7, 8, and globin. The role of cross-linked membrane protein polymers in the generation of ISCs is discussed and is synthesized in terms of a unified concept for the determinants of the genesis of ISCs.

Key words: irreversibly sickled cells, freeze-etching, scanning electron micrography, membrane-bound hemoglobin, membrane proteins and glycoproteins

The irreversibly sickled cell (ISC), a dense, rigid bipolar cell which can be isolated from the blood of sickle cell patients has been shown to contribute to the abnormal rheologic properties of oxygenated sickle cell blood. Visualization of sickle cells through the microvasculature of animal models suggests that ISCs may initiate microvascular occlusion and thus play an important pathophysiologic role in the generation of the vasooclusive crises [1]. Although the rheologic abnormality of the ISC has been attributed to alterations

Received May 4, 1978; accepted August 4, 1978.

0091-7419/78/0904-0537$03.20

of its membrane, the precise nature of the biochemical lesion in terms of rearrangement of macromolecular architecture has not been elucidated. A minor controversy has arisen regarding the origin of the ISCs. Some studies suggest that ISCs emerge from the bone marrow of sickle cell patients with low hemoglobin F and thus are predestined to undergo rapid membrane alteration and shortened circulatory survival [2, 3]. Studies of in vitro production of ISCs from our laboratory and others indicate that the membrane alteration in the ISC is a cumulative, progressive change [4–7]. We have previously shown that when sickle cells are incubated under anoxic conditions, there is progressive accumulation of membrane-bound hemoglobin [4]. Padilla et al [6] demonstrated that ISCs may be generated by repetitive sickling and unsickling of individual sickle cells with progressive membrane loss by microspherulation. In a preliminary study we have shown that with repetitive sickling and unsickling, there is selective loss of hemoglobin F from sickle cells by microspherulation [8]. This may occur because hemoglobin F does not copolymerize with hemoglobin S in the deoxygenated state [9] and thus is rapidly lost from the cell surface within vesicles which fragment during unsickling. Eaton et al [10] and Palek [11] have shown that sickle cells manifest accumulation of calcium within the cell, with a significant fraction bound to the membrane. Lux and co-workers [12], utilizing Triton-extracted membrane residues of ISCs have demonstrated that the shape alteration of the ISC is conferred by irreversible changes within the "spectrin-actin lattice." It is our contention that these events work together to bring about a progressive and cumulative alteration in the membrane of sickle cells as their shape and deformability become irreversibly altered in the generation of the ISC.

In the present study, ISCs were obtained from two sources: 1) in vivo ISCs were derived from centrifugal separation of whole blood of sickle cell anemia patients in which greater than 90% of the total ISC content is localized in the 15% bottom fraction, and 2) ISCs were produced in vitro by incubation under anoxic conditions for up to 24 h, with and without adenosine triphosphatase (ATP) depletion. These studies have been designed to permit concomitant observation of ISC membrane changes, both morphologically and biochemically. They employed scanning electron microscopy, freeze-etching with transmission electron microscopy, and histochemical staining of membranes for hemoglobin. Cells obtained from the same experiments are subjected to concomitant analyses for membrane associated hemoglobin, ATP, 2,3-diphosphoglycerate (2,3-DPG), age-dependent enzymes, and sodium dodecyl sulphate (SDS) polyacrylamide gel electrophoresis of their membrane proteins and glycoproteins.

METHODS

Preparation of Red Cells and Membranes

Fresh blood was obtained by venipuncture from normal control (AA) subjects and individuals with sickle cell anemia (SS). The blood was anticoagulated with sodium heparin (14 units/ml). Hemoglobin genotypes of the patients were verified by cellulose acetate (pH 8.4) and citrate agar (pH 6.4) electrophoresis. Hemoglobin F levels were determined by the alkaline denaturation technique [13]. Blood specimens were drawn from the patients during clinical steady states, and hematocrit values ranged from 25% to 40%.

Hemoglobin-free red cell membranes were prepared by the method of Dodge et al [14] using 20 mOsm Tris-HCl buffer, pH 7.6. Membranes were used in various analyses, including residual hemoglobin [15], as soon as possible. Membranes not immediately used for assays were stored at −70°C.

Electron Microscopy

Cells or membrane preparations for electron microscopy were fixed in 1% glutaraldehyde in phosphate buffer (pH 7.4) and processed by the method of Bessis and Weed [16] for scanning electron microscopy (SEM). Samples for transmission electron microscopy (TEM) were fixed in 1% glutaraldehyde, washed twice with buffer, postfixed in 1% osmium tetroxide in phosphate buffer (pH 7.4), dehydrated in graded ethanol, and embedded in Epon 812. Thin sections were stained with uranyl acetate and lead citrate [17] and examined in an AEI EM 801 transmission electron microscope.

Freeze-Etching

Freeze-etching was carried out in a Balzers 360M ultra-high-vacuum device by the method previously described [18]. After the initial red cell or membrane preparation procedures, cells or membranes were cryoprotected in serial glycerol solutions to final concentrations from 25 to 40% in phosphate-buffered saline (pH 7.4). Droplets of cell suspension were then frozen on gold disks in liquid Freon 22 (−160°C) and stored in liquid nitrogen. Specimens were placed on the freeze-etching microtome stage and the chamber was evacuated to 10^{-6} torr. The specimen was then fractured by a single stroke or multiple chips using the cold (−100°C) microtome blade and sublimated (etched) for periods of time varying from one to ten minutes. The replica was produced by evaporation of platinum and carbon onto the fractured surface. The replica was removed from the freeze-etching device, cleaned of cellular debris by flotation in distilled water, 70% sulfuric acid, and dilute sodium hypochlorite, and rinsed in distilled water. Replicas thus obtained were studied and photographed in an AEI EM 801 electron microscope at 10,000–40,000 times magnification.

Incubation of Sickle Cells and the Determination of ISCs

Normal and sickle cells were incubated for 24 h in isoosmotic Krebs-Henseleit buffer of the following composition in mM: NaCl 110, KCl 5.9, $CaCl_2$ 2.0, $MgSO_4 \cdot 7H_2O$ 1.2, $NaH_2PO_4 \cdot H_2O$ 2.4, $NaHCO_3$ 25.0, glucose 30.0, bovine serum albumin 0.51% (pH 7.4, 290 mOsm) under 95% O_2 or 95% N_2 with 5% CO_2. Cells were sampled at intervals for determination of %ISCs, ATP, membrane-bound hemoglobin, Na^+, and K^+, and for freeze-etch and transmission EM of whole cells and membrane preparations.

Differential Centrifugation of Sickle Cells

In vivo ISCs were isolated from freshly packed sickle cell blood by ultracentrifugation for 1 h at 100,000g and fractionated into bottom 15%, middle 70%, and top 15% of the densely packed cells. Various analytical procedures and chemical determinations were performed on these cell fractions.

Morphologic Characterization of Irreversibly Sickled Cells

ISCs were defined as Hb-SS cells with one or more pointed extremities under oxygenated conditions, as defined by Jensen et al [19].

Analytical Procedures

ATP content of cell preparations were determined by the method of Kornberg [20] as modified by Lamprecht and Trautschold [21] by enzymatic determination of neutralized perchloric acid extracts. 2,3-DPG was determined by the method of Rose and Liebowitz [22]. Intracellular sodium and pottassium were analyzed as described elsewhere [23]. Membrane-bound hemoglobin was analyzed histochemically by the method of Breton-Gorius using diaminobenzidine [24]. Membrane-bound hemoglobin was determined for 20-μl aliquots of membrane preparation employing the benzidine reaction method of Crosby and Furth [15].

Electrophoresis of membrane proteins and glycoproteins in 5.6% polyacrylamide gels with 0.2% bis-acrylamide as cross-linker in 1% sodium dodecyl sulfate was executed as described by Fairbanks et al [25]. Each gel was loaded with 30 μg protein. Membrane proteins were determined by the method of Lowry et al using bovine serum albumin as a standard [26]. After electrophoresis, gels were stained for protein with Coomassie Blue R-250 and for protein-bound carbohydrate with periodic acid-Schiff (PAS) reagent and were photographed through a medium red filter (Kodak #25). Densitometry was performed at 560 nm using a Beckman ACTA CIII spectrophotometer.

RESULTS

Ultrastructural Studies

Scanning electron microscope observations. ISCs obtained from whole blood of SS patients by ultracentrifugation have a characteristic shape (Fig. 1A–C). They are fusiform cells in the shape of crescents with two pointed extremities. The membrane surface of the ISC in the oxygenated state is often irregular but without visible organization. In the deoxygenated state the surface of the ISC tends to reflect polymerization of submembrane deoxyhemoglobin S with the presence of subsurface fibers and irregular indentation of the membrane (Fig. 1D). ISCs produced in vitro by an anoxic incubation show a different shape abnormality from those isolated from blood of SS patients. In vitro ISCs show a much greater degree of spiculation and membrane distortion, often displaying multiple spicules and holly-leaf (drepanoechinocyte) configurations. These cells appear to have arisen from echinocytic forms. Both in vitro and in vivo ISCs show evidence of membrane loss by fragmentation.

Freeze-etching and transmission electron microscopy. Freeze-etch electron micrographs of ISCs and their membranes isolated by hypotonic lysis and centrifugation show the accumulation of microbodies on the internal membrane (PS) surface (Fig. 2A,B). These microbodies measure ca. 50 × 10 nm and show a random distribution over what appears to be the internal membrane (PS) surface. The microbodies obscure filamentous structures usually visible on the PS surface. In some preparations, the microbodies appear to be associated with a rearrangement of membrane-associated particles on the intramembrane (PF) surface. In vivo ISCs isolated from whole blood of SS patients show similar microaggregates on the internal (PS) aspect of the ISC membrane. In some cases, aggregates of this material seen in cross-section in the submembrane region resemble small Heinz bodies (Fig. 3A). The degree of microaggregate formation is less prominent within in vivo than in vitro ISCs. When ISCs are generated by repetitive sickling and unsickling, the

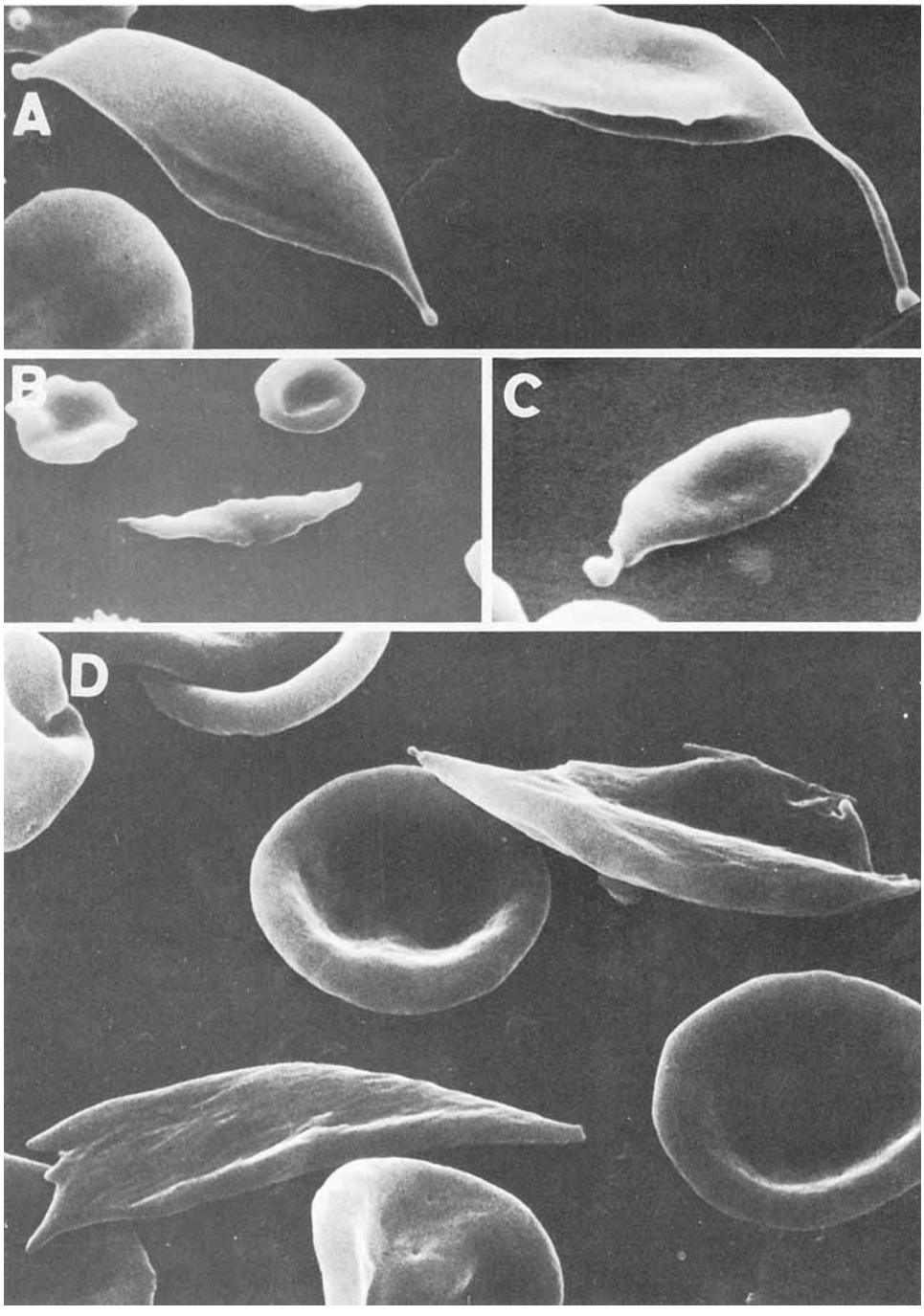

Fig. 1. Scanning electron micrographs of ISCs isolated from whole SS blood by ultracentrifugation. Cells were prepared as described in Methods [16]. Final magnification A ≃ 10,000 × B, C ≃ 4,000 ×, D ≃ 10,000 ×.

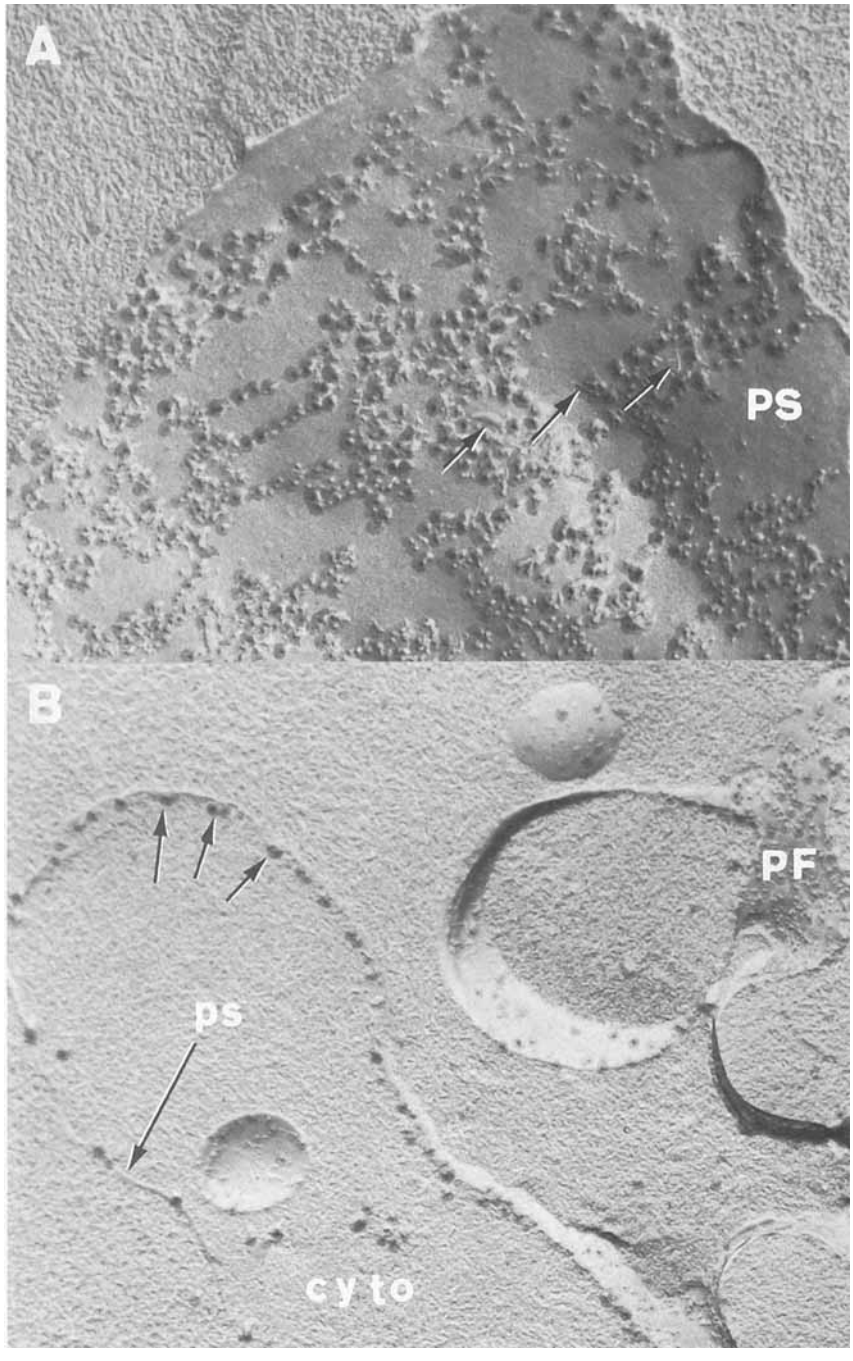

Fig. 2. Freeze-etch electron micrographs of ISCs showing microbodies on the internal (PS) surface of the membrane and the aggregation of intermembranous particles on the PF surface. Note the marked distortion of the PS surface by large numbers of adherent microbidies. Filamentous structures can also be seen (A, arrows). Alignment of microbodies along the PS surface is also clear in the cross section (B). Cyto = cytoplasm. Final magnification: A = 100,000 ×, B = 100,000 ×.

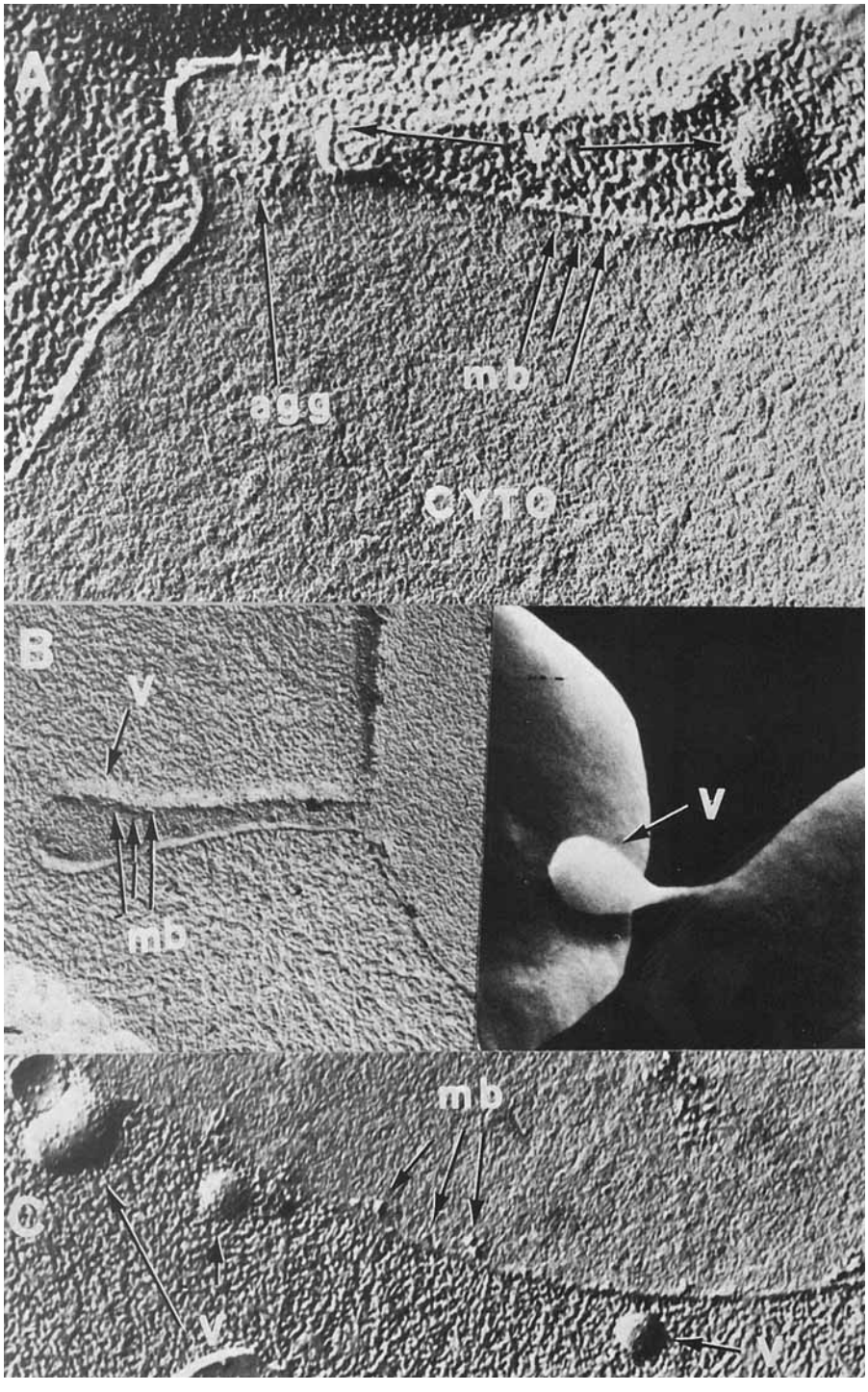

Fig. 3. Freeze-etch A, B left, C) and scanning electron micrograph (B right) of ISCs produced in vitro, showing the development of membrane-associated hemoglobin aggregates (agg) and their relationship to membrane loss by vesiculation (V). Submembrane microbodies (mb) are visible at cytoplasm-PS interfaces. Cyto = cytoplasm. Final magnification: A = 40,000 ×, B (left) ≃ 40,000 ×, B (right) = 20,000 ×, C = 40,000 ×.

development of submembrane microaggregates is shown to accompany the fragmentation process (Fig. 3A–C). Aggregates occur initially in the region of the retracting spicules during the unsickling process and appear to play a role in fragmentation and microvesiculation, perhaps by annealing apposing internal membrane (PS) surfaces, thus fostering disjunction of the vesicle from the main body of the cell (Fig. 3B,C).

In order to determine the nature of the submembrane aggregates, ISCs produced in vitro by anoxic incubation (with increased membrane-associated hemoglobin and decline of ATP levels) were subjected to hypotonic lysis and stained histochemically for hemoglobin with diaminobenzidine (DAB). Figure 4A shows control membranes in which no membrane-bound hemoglobin is visible. Figure 4B represents DAB-stained membranes of in vitro ISCs and shows numerous aggregates of submembrane DAB-positive material. This suggests that the submembrane aggregates seen in such preparations are hemoglobin or derivatives of hemoglobin.

In Vitro Production of ISCs and Binding of Hemoglobin to ISC Membranes

ISCs were produced by incubation for 24 h in isotonic Krebs-Henseleit buffer under 95% N_2 with 5% CO_2, with continuous shaking in an oscillating waterbath at 37°C. Control sickle cells were incubated with 95% O_2/5% CO_2 and control normal cells were incubated under identical oxygenated and anoxic conditions. Cells incubated 0–24 h were sampled at intervals for determination of percentage of ISCs, ATP, and membrane-bound hemoglobin, as well as freeze-etch and transmission electron microscopy. As indicated in Figure 5A, ISC generation from SS cells during the 24-h incubation showed a sigmoid curve with gradual increment in the initial 8 h, a sharp rise during the second 8-h period, and plateauing in the final 4 h. ATP levels were maintained in oxygenated SS and control cells for the entire incubation, but fell slightly in SS cells after 16 h under deoxygenated conditions (Fig. 5B). Membrane-bound hemoglobin showed a 100-fold increase during the 24-h incubation, rising from 2 mg% to 250 mg%, as indicated in Fig. 6. Incubated control AA cells and oxygenated SS cells showed no appreciable accumulation of hemoglobin with the membrane fraction.

In the ATP maintenance experiments, shown in Fig. 7, membrane-bound hemoglobin rose from 40 mg% to 90 mg%, whereas no significant rise was seen in SS cells incubated under oxygen, or in control cells. In both experiments, whether ATP was allowed to fall or was maintained, a significant fall in cellular potassium and a concomitant rise in cellular sodium occurred in the SS cells incubated under N_2, whereas control sickle and normal cells under O_2 showed only minor alterations in intracellular potassium and sodium.

Chemical Characterization of ISCs Isolated From Blood of SS Patients

Whole blood from sickle cell patients was fractionated by ultracentrifugation at 100,000g for 1 h and cells were separated into the upper 15% "reticulocyte-rich" fraction, a middle 70% non-ISC fraction, and a bottom 15% "ISC-rich" fraction. Table I shows data from a representative separation, with determinations of ATP, 2,3-DPG, pyruvate kinase (an age-dependent enzyme) activity, cellular sodium, and membrane-associated hemoglobin. Values for normal control AA erythrocytes subjected to similar analysis are also shown. The ISC fraction shows membrane-associated hemoglobin to be three times greater than the middle (non-ISC) fraction. The reduction in ATP level seen in the ISCs is significant but does not represent total depletion and should not substantially impair cellular functions dependent upon the availability of high-energy phosphate. The high level of membrane-associated hemoglobin seen in reticulocytes is an expected finding because of continued hemoglobin synthesis in polyribosomes associated with the reticulocyte membrane [27].

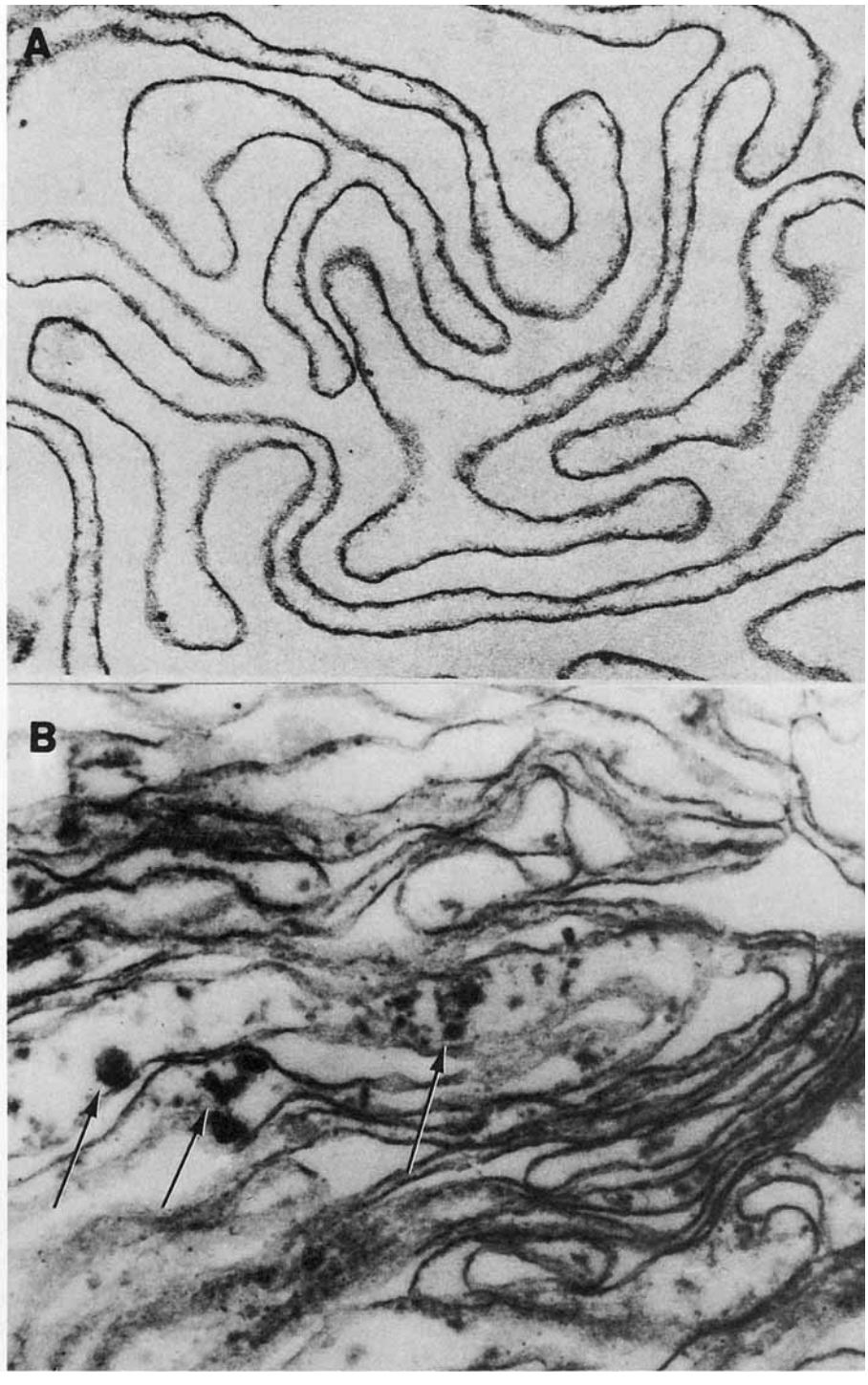

Fig. 4. A) Electron micrograph of purified SS cell membranes isolated from whole blood without anaerobic incubation of cells. The micrograph shows the richness of the preparation, and the minimal residual heme compounds associated with the membranes. B) SS cell membranes isolated from cells incubated under anaerobic conditions (95% N_2, 5% CO_2, 37°C, 12–18 h). Membranes were stained with diaminobenzidine [24]. Dark membrane-associated clumps represent hemoglobin and/or its derivatives. Final magnification = 25,000 ×.

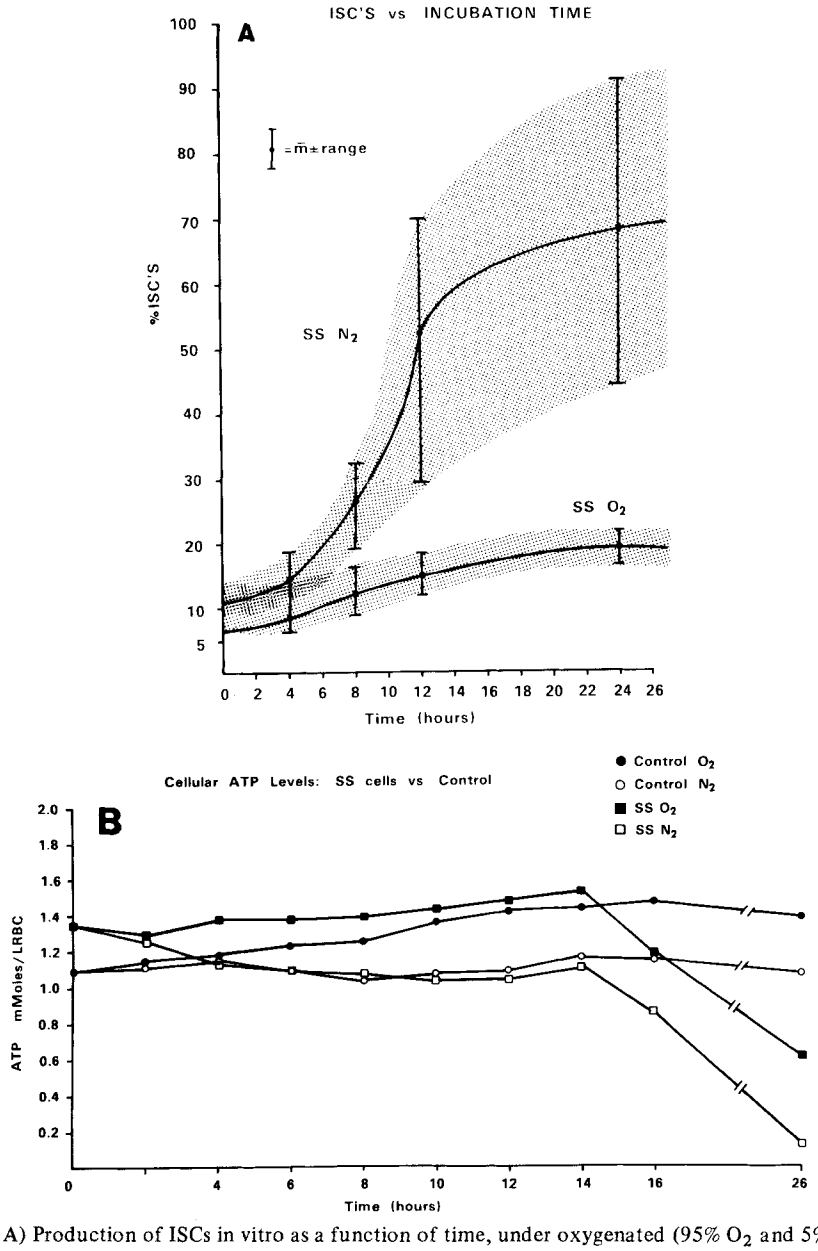

Fig. 5. A) Production of ISCs in vitro as a function of time, under oxygenated (95% O_2 and 5% CO_2) and deoxygenated (95% N_2 and 5% CO_2) conditions. Incubation conditions are described in Methods. B) Intracellular ATP concentration of AA and SS erythrocytes during in vitro production of ISCs. Graph represents mean of three determinations. For details see Methods. Note the early decline of ATP concentrations in the SS cells.

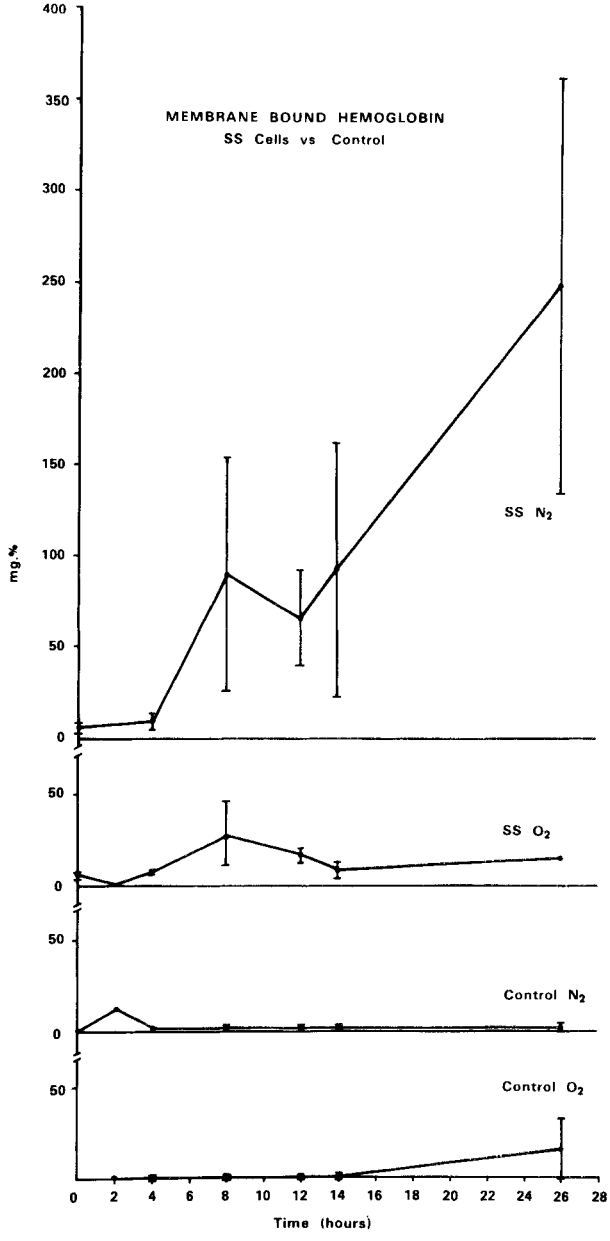

Fig. 6. Membrane-bound hemoglobin of control (AA) and sickle cells (SS) as a function of time during incubation under oxygenated (95% O_2 and 5% CO_2) and deoxygenated (95% N_2 and 5% CO_2) conditions. Ordinate expressed as mg% of hemoglobin from a standard curve; 20 μl of ghost suspension used for assay.

SDS Polyacrylamide Gel Electrophoresis Analysis of ISC Membranes

When cells from top, middle, and bottom fractions are lysed and their membranes are solubilized with sodium dodecyl sulfate and electrophoresed in SDS-polyacrylamide gels after reduction of protein disulfide bonds with dithiothreitol, significant differences are evident between the membranes from non-ISC and ISC fractions, as shown in Fig. 8A. The membrane protein and glycoprotein profile of membranes from the non-ISC fraction does

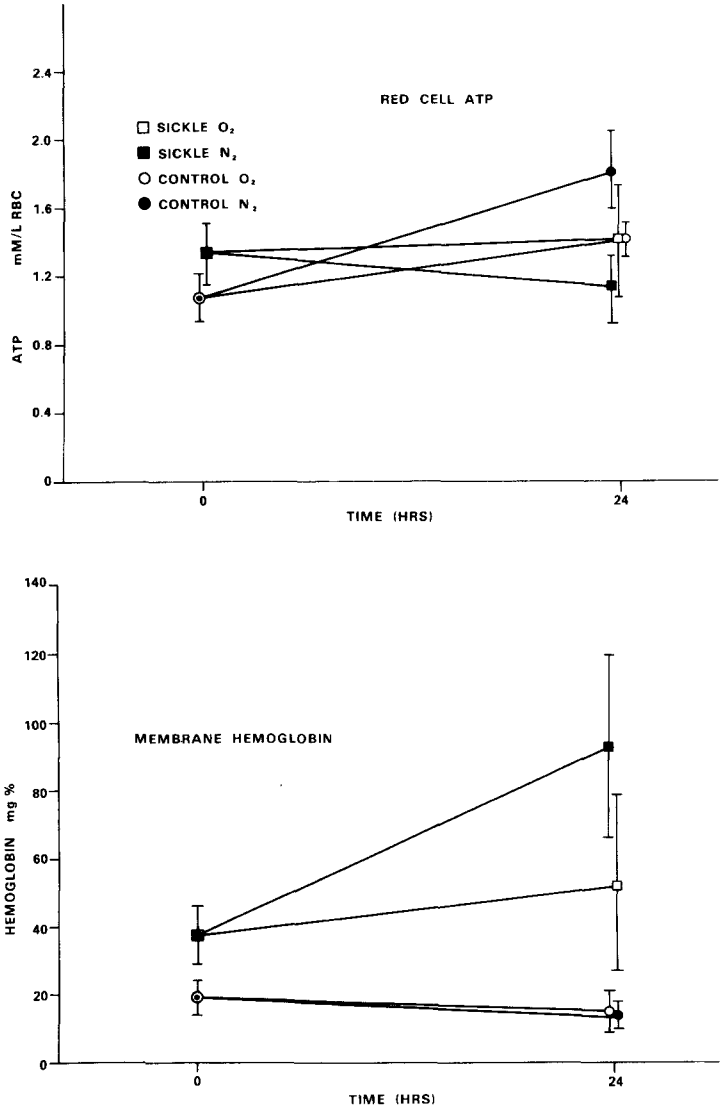

Fig. 7. Above) ATP concentrations of control (AA) and sickle cells (SS) before and after incubation under oxygenated and deoxygenated conditions. Below) Membrane-bound hemoglobin of normal (AA) cells and sickle cells (SS) before and after incubation under oxygenated and deoxygenated conditions. Ordinate expressed as mg% of hemoglobin from a standard curve. A 1-ml aliquot of ghost suspension was used for assay; final data are expressed as mg% Hb for a liter of ghosts, taking into account the packed cell volume used.

TABLE I. Separation of Sickle Cell Fractions by Ultracentrifugation Comparison With Control AA Red Cells

	Hct %	ATP (mmoles/ liter RBC)	2,3-DPG (mmoles/ liter RBC)	Pyruvate kinase (EU/gmHb)	Na (mmoles/ liter RBC)	Membrane Hb (mg%)	Retics (%)	ISC (%)
Sickle								
Top	0.4195	1.93	5.67	15.32	7.3	74.5	97.5	6.3
Middle	0.4288	1.48	7.92	4.14	8.2	18.5	–	6.4
Bottom	0.3927	1.17	5.51	3.13	33.3	49.9	3.6	62.0
Control								
Top	0.4781	1.24	4.75	3.49	9.4	70.5	3.2	0
Middle	0.3683	1.24	4.88	1.75	11.1	26.6	–	0
Bottom	0.1908	1.23	3.70	1.46	14.1	26.0	0	0

Packed red cells from fresh sickle cell blood was fractionated, by ultracentrifugation at 100,000g for 1 h, into reticulocyte-rich (top 15%), non-ISC (middle 70%), and ISC fractions (bottom 15%). The table shows a 62% ISC yield in the bottom fraction and characterizes the in vivo ISC as a cell with low ATP and pyruvate kinase, increased sodium, and high membrane-bound hemoglobin.
EU, Enzyme Units = Activity of enzyme as μmole substrate transformed per minute per gm Hb.

not differ significantly from the SDS polyacrylamide gel electrophoresis (PAGE) pattern seen in normal erythrocytes. In the ISCs, however, several important differences can be seen. There is a marked increased in the globin band, presumably derived from the membrane-associated hemoglobin of the ISCs. Band 4.1 has decreased staining intensity, whereas bands 7 and 8 were increased. At the pre–band 1 region of the gel were high-molecular-weight complexes (greater than 270,000–280,000 daltons) which may be heteropolymers of certain low-molecular-weight proteins. The exact nature of these heteropolymers was not determined in the present study. No differences were observed in the glycoprotein (PAS) bands (Fig. 8, right panel). Figure 9 illustrates representative densitometric scans of the stained polyacrylamide gels. Reticulocytes also show an increase in membrane-associated globin by this method, as well as high-molecular-weight complexes which may represent membrane-associated ribosomal material. There is no decrease, however, in band 4.1 in the reticulocyte membrane fraction.

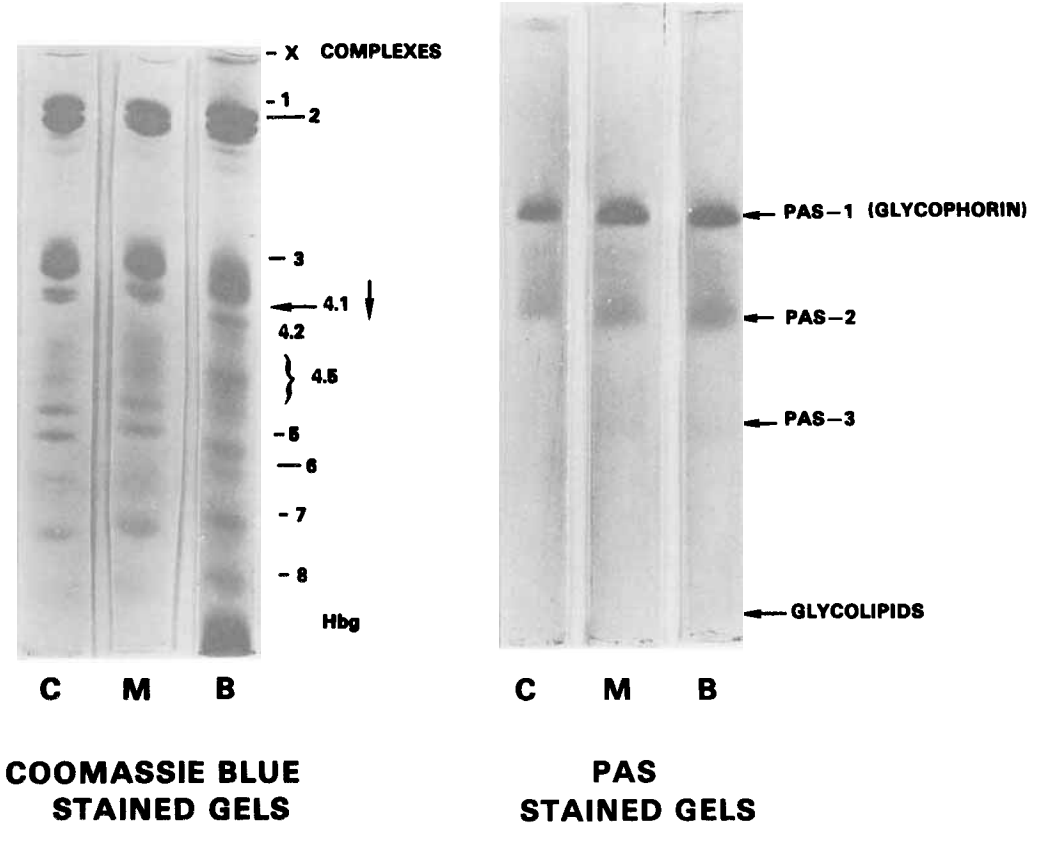

Fig. 8. Sodium dodecyl sulfate and polyacrylamide gel electrophoretograms of red cell ghost proteins from normal controls (C), middle fraction of packed sickle cells (M), and bottom fraction of packed sickle cells (B). Ghosts [14] were dissolved in 1% SDS, 0.1% dithiothreitol, and buffer, incubated at 37°C for 30 min, and electrophoresed as described in Methods [25]; 30 μg protein was loaded on each gel. Gels were stained with Coomassie Blue for the proteins (left); and periodic acid-Schiff reagent (PAS) for the glycoproteins (right). The top fraction of packed sickle cells is not included because of the high proportion of reticulocytes.

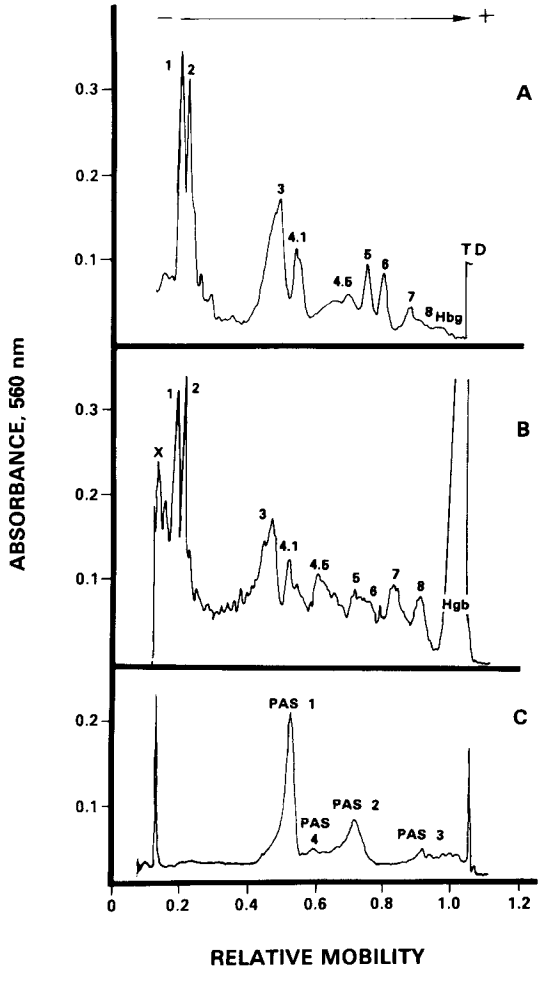

Fig. 9. Densitometric scans of Coomassie Blue-stained proteins of control cell membranes (A), and bottom fraction of packed sickle cell membranes (ISC-rich) (B). The scan of the PAS-stained gel (C) represents the common profile observed in both control cells and fractionated sickle cell membranes. Note the presence of all four bands, PAS 1, 2, 3, and 4, as previously described [25].

DISCUSSION

Using concomitant ultrastructural and biochemical methods, we have assessed the membrane alteration both in ISCs isolated in vivo and in ISCs generated in vitro. Morphologically, the ISC is a bipolar fusiform cell with two or more pointed excrescences, often showing microspherulation from the extremities of the cell. When deoxygenated, the ISC does not undergo a basic shape change, but shows membrane surface (ES) alterations which reflect the polymerized state of submembrane deoxyhemoglobin S. ISCs produced in vitro show shape and membrane alterations similar to those found in in vivo ISCs; however, distortions are much more marked and the cells appear to have arisen from echinocytic forms, thus assuming drepanoechinocyte shapes. Cell membrane loss by vesiculation is a

common finding in both in vitro and in vivo ISCs. Vesiculation of sickle cells during unsickling [6] and upon agitation in the deoxygenated state [28] leads to net membrane loss which further contributes to ISC generation.

We have previously reported that freeze-etching and TEM of ATP-depleted ISCs revealed microbodies on the internal membrane (PS) surface [4, 18]. These microbodies distort intramembrane PF and EF surfaces at sites containing intramembranous particles (IMPs). Submembrane microbodies are accompanied by aggregation of IMPs on the overlying PF surface, which suggests binding of microbodies to intrinsic membrane proteins. When in vivo ISCs are examined as whole cells or ghosts, microbodies similar to those seen in the in vitro ISCs can be readily identified. However, they appear less numerous, and appear to be present at the membrane-cytoplasm interface (PS), where they are associated with aggregated IMPs on the PF surface. When the in vivo ISC is subjected to a single cycle of deoxygenation-reoxygenation, submembrane microbodies appear in the region of the spicules, from which segments of the membrane are lost by vesiculation [18]. The association of microbody formation with membrane loss by vesiculation is morphologically evident. Most vesicles that are seen in cross-section contain microaggregates which in some way foster the loss of vesicles from the cell. We therefore postulate that the interaction of deoxyhemoglobin S with membrane proteins may serve to anneal apposing internal membrane (PS) surfaces and thus lead to formation of vesicles from the cell.

EM histochemistry of ISC membranes has demonstrated that submembrane aggregates found only in the ISC fraction were diaminobenzidine-positive, indicating the presence of hemoglobin and/or hemoglobin derivatives. Increased content of methemoglobin has been demonstrated in sickle cells, and recently Asakura et al [29] have shown spectrophotometrically that the heme compounds associated with membranes of sickle cells are predominately methemoglobin [29]. Fischer et al [30] have found increased "retention" of hemoglobin in membranes of ISCs compared to normal cells.

ISCs produced in vitro by anoxic incubation [31] acquired increasing amounts of membrane-associated hemoglobin. This membrane hemoglobin was not observed in AA and SS control cells and occurred prior to substantial ATP depletion. Similar experiments with an ATP-maintenance medium demonstrated that membrane-associated hemoglobin in ISCs increased irrespective of intracellular ATP levels and that simultaneously intracellular sodium and potassium concentrations were altered. Other studies have demonstrated that during anoxic incubation of sickle cells, calcium accumulation occurs largely in the membrane fraction, and correlates directly with ISC content [11].

Our results, and current studies of the ISC membrane, suggest that the acquired defect of the ISC membrane lies in the protein components [4, 12, 34–36]. Durocher and Conrad [32] reported that the SDS PAGE protein profiles from AA and SS membranes are similar, and others have made similar observation [33]. By contrast, Riggs and Ingram [34] found decreases in bands 1, 2, 2.2, 2.3, and 3, and increases in bands 4.5, 6, 7, and globin, as well as a marked decrease in sialic acid content of SS cell membranes. Lux et al [12], studying Triton X-100-extracted ghosts of ISCs, found that the membrane residues retained the shape of the original ISC and suggested that the defective morphology of the ISC probably lies in the "spectrin-actin lattice." In our studies of ISCs isolated in vivo, SDS PAGE revealed significant differences between ISCs and non-ISC fractions. The marked increase in the globin band in the Coomassie Blue-stained gels is consistent with the increase in membrane-associated hemoglobin shown by the other methods. The decrease in band 4.1 may be due to the involvement of these proteins in the formation of the pre–band 1 heteropolymer. Although the components of this high-molecular-weight complex have not

been determined in the present study, cross-linking studies of AA cell membranes using diamine (diazine dicarboxylic acid bisdimethylamide) [39] suggest that proteins such as bands 1, 2, 3, and 4.1 may be components of the pre–band 1 heteropolymer. Palek et al [35], employing catalytic oxidation of protein SH groups, found that ISC membrane proteins formed a 450,000-dalton complex of spectrin 1 + 2, a 260,000-dalton complex of bands 2 + 4.9, and a small amount of bands 3 and actin dimers. Lorand and co-workers [36] have attributed the formation of high-molecular-weight complexes within normal (AA) membranes in the presence of calcium [37, 38] to protein cross-linking mediated by a transglutaminase. Lorand et al [36] suggest that calcium influx into the red cell activates this enzyme, which would conceivably induce the cross-linking of membrane proteins by means of γ-glutamyl–ϵ-lysine bridges. Formation of these cross-linked polymers is generally accompanied by reduction in band 4.1 [36, 38, 39], suggesting the involvement of this band in the polymerization. The relation of these membrane protein heteropolymers to the microbodies observed in ISC membranes is at present unknown. However, variations in experimental conditions such as electrophoresis, staining, and destaining procedures may influence the resultant gel pattern and explain the divergent findings from several laboratories.

The ISC has a markedly decreased cellular deformability as demonstrated by micropipette elastimetry [5], cell filtration [40, 41], and viscometric studies [42]. This alteration in deformability is due to increased membrane rigidity [5, 43]. The chemical basis for this alteration in the biophysical characteristics of the ISC membrane may be considered in terms of alteration of molecular organization of the ISC. It has been our contention that the membrane defect of the ISC is an acquired cumulative or progressive lesion in which several factors can be identified and synthesized into a unified concept: 1) Deoxyhemoglobin S or denatured hemoglobin S binds to the membrane of the ISC. 2) This deoxyhemoglobin S–membrane interaction is associated with an apparent increase in membrane and cellular calcium in the ISC, and may occur independently of alteration in cellular ATP level. 3) The association of deoxyhemoglobin S and calcium with the membrane may be indicators of alterations in the macromolecular (protein) organization of the membrane, rather than principal events in the generation of the ISC membrane lesion. 4) The irreversible shape alteration in the ISC and perhaps its membrane rigidity can be attributed to irreversible cross-linking or protein components, perhaps through disulfide bridges, of the spectrin-actin lattice of the cell membrane. 5) This cross-linking may be mediated by a calcium-dependent transglutaminase enzyme and explain the presence of high-molecular-weight complexes found in polyacrylamide gel electrophoresis patterns of ISC membranes.

ACKNOWLEDGMENTS

This study was supported in part by contract No. N01-HL-2-2946B from the National Heart and Lung Institute, and a World Health Organization Fellowship to J. Kurantsin-Mills.

The authors thank Mr Frank Stewart, departmental secretary, for his assistance in typing the manuscript and the Audio-Visual Division of the George Washington University Medical Center for processing illustrations.

REFERENCES

1. Klug PP, Lessin LS, Radice P: Arch Intern Med 133:577, 1974.
2. Bertles JF, Milner PFA: J Clin Invest 47:1731, 1968.

3. Sergeant GR, Sergeant BE, Milner PFA, Br J Haematol 17:527, 1969.
4. Lessin LS, Wallas C: Blood 42:978, 1973.
5. Havell T, Hillman D, Lessin LS: Am J. Hematol 4:9, 1978.
6. Padilla F, Bromberg PA, Jensen WN: Blood 41:653, 1973.
7. Palek J: Blood 42:988, 1973.
8. Yoo D, Lessin LS, Jensen WN: Clin Res 23:285, 1975.
9. Bookchin RM, Nagel RL: Sem Hematol 11:577, 1974.
10. Eaton J, Skelton T, Swofford H, Kolpin C, Jacob H: Nature 246:105, 1973.
11. Palek J: J Lab Clin Med 89:1365, 1977.
12. Lux SE, John KM, Karnovsky MJ: J Clin Invest 58:955, 1976.
13. Singer K, Chernoff AI, Singer L: Blood 6:413, 1951.
14. Dodge JT, Mitchell C, Hanahan DJ: Arch Biochem Biophys 100:119, 1963.
15. Crosby WH, Furth FW: Blood 11:380, 1956.
16. Bessis M, Weed RI: In Johari O, Corvin I (eds): "Scanning Electron Microscopy, Part II." Chicago: Illinois Institute of Technology Research Institute, 1972, p 289.
17. Reynolds ES: J Cell Biol 17:208, 1963.
18. Lessin LS: Nouv Rev Franc Hematol 12:151, 1972.
19. Jensen WN, Ruchnagel DL, Taylor WJ: J Lab Clin Med 56:854, 1960.
20. Kornberg A: J Biol 182:779, 1950.
21. Lamprecht W, Trautschold I: In Bergmeyer HU (ed): "Methods in Enzymatic Analysis." New York: Academic, 1974, p 2101.
22. Rose ZB, Liebowitz J: Anal Biochem 35:177, 1970.
23. Kurantsin-Mills J, Kudo M, Addae SK: Clin Sci Mol Med 46:679, 1974.
24. Breton-Gorius J: Nouv Rev Franc Hematol 10:243, 1970.
25. Fairbanks G, Steck TL, Wallach DFH: Biochemistry 10:2606, 1971.
26. Lowry OH, Rosebrough NJ, Farr AL, Randall RJ: J Biol Chem 193:265, 1951.
27. Bessis M: "Living Blood Cells and Their Ultrastructure." New York: Springer-Verlag, 1973, p 134.
28. Bessis M, Bricka M: Rev Hematol 7:407, 1952.
29. Asakura T, Minakata K, Adachi K, Russel MO, Schwartz E: J Clin Invest 59:633, 1977.
30. Fischer S, Nagel RL, Bookchin RM, Roth EF, Tellez-Nagel I: Biochem Biophys Acta 375:422, 1975.
31. Shen SC, Fleming EM, Castle WB: Blood 4:498, 1949.
32. Durocher JR, Conrad ME: Proc Soc Exp Biol Med 146:373, 1974.
33. Dzandu J, Johnson RM: J Supramol Struct (Suppl) 2:209, 1978.
34. Riggs MG, Ingram VM: Biochem Biophys Res Commun 74:191, 1977.
35. Palek J, Liu SC, Liu A: In Kruckeberg WC, Eaton JW, Brewer GJ (eds): "Progress in Clinical and Biological Research." New York: Alan R Liss, 1978, vol 20.
36. Lorand L, Weissman LB, Epel DL, Bruner-Lorand J: Proc Nat Acad Sci USA 73:4479, 1976.
37. Carraway KL, Triplett RB, Anderson DR: Biochim Biophys Acta 379:571, 1975.
38. King LE, Morrison M: Biochim Biophys Acta 471:162, 1977.
39. Kurantsin-Mills J, Lessin LS: Biophys J 21:119a, 1978.
40. Lessin LS, Kurantsin-Mills J, Weems HB: Blood Cells 3:241, 1977.
41. Lessin LS, Kurantsin-Mills J, Klug PP, Weems HB: In Kruckeberg WC, Eaton JW, Brewer GJ (eds): "Progress in Clinical and Biological Research." New York: Alan R Liss, 1978, vol 20.
42. Chien S, Usami S, Bertles J: J Clin Invest 49:623, 1970.
43. LaCelle PL: Blood Cells 1:269, 1975.